Electron-impact dissociative ionization of the molecular ion HDO^+: A global view

P. Defrance
Catholic University of Louvain, Institute of Condensed Matter and Nanosciences, Chemin du Cyclotron 2, 1348 Louvain-la-Neuve, Belgium

J. Jureta
Catholic University of Louvain, Institute of Condensed Matter and Nanosciences, Chemin du Cyclotron 2, 1348 Louvain-la-Neuve, Belgium and Institute of Physics, University of Belgrade, P. O. Box 68, 11081, Belgrade, Serbia

J. Lecointre
Haute Ecole Namur-Liège-Luxembourg HENALLUX, Département Ingénieur Industriel, Pierrard, Rue d'Arlon 112, B-6760 Virton, Belgium

E. Giglio and B. Gervais
CIMAP, Unité Mixte CEA-CNRS-ENSICAEN-UCBN 6252, BP 5133, F-14070 Caen, Cedex 05, France

C. Dal Cappello and M. Ruiz-Lopez
SRSMC, UMR CNRS 7565, University of Lorraine, BP 70239, 54506 Vandoeuvre-les-Nancy, France

I. Charpentier
Icube - UMR 7357, Laboratoire des sciences de l'ingénieur, de l'informatique et de l'imagerie 300 bd Sébastien Brant - CS 10413 - F-67412 Illkirch Cedex, France

P.-A. Hervieux
Institut de Physique et Chimie des Matériaux de Strasbourg, CNRS and Université de Strasbourg BP 43, F-67034 Strasbourg, France
(Received 17 July 2014; published 10 October 2014)

We present a combined experimental and theoretical study of the fragmentation of HDO^{2+} molecular ions produced by electron-impact ionization of HDO^+ in the collision energy range 20–2500 eV. Experimental absolute partial inclusive cross sections for the production of OD^+, OH^+, and O^+ are reported and compared successfully to theoretical predictions. *Ab initio* methods are used to calculate the electron-impact ionization cross sections of the cationic ground state and first excited state leading to the first seven dicationic states. Dissociation probabilities of each channel are obtained by performing classical molecular dynamics on fitted dicationic potential energy surfaces. The predictive character of the theoretical modeling allows us to estimate that the nonmeasured dissociation channel giving a neutral oxygen atom contributes to 30% of the total ionization cross section. The isotopic ratio OD^+/OH^+ deduced from the experiment is (3.1 ± 0.2) on average, constant in the 30–2500 eV energy range. The calculated isotopic ratio is found to be strongly dependent on the vibrational excitation of the target. Good agreement with the experimental value is obtained for a vibrational excitation corresponding to a temperature of about 2500 K, which is compatible with typical characteristics of electron cyclotron resonance (ECR) ion sources.

DOI: 10.1103/PhysRevA.90.042704 PACS number(s): 34.80.Gs

I. INTRODUCTION

Understanding the fragmentation dynamics of excited or/and charged molecular systems is a very active and fascinating domain of research. Many relaxation processes are possible depending on the system, its internal energy, and its charge state, even for molecular systems having a relatively small number of degrees of freedom. Moreover, these processes may compete and occur on different time scales ranging from femtoseconds to seconds. When the dissociation is induced by projectile impact, it is therefore extremely difficult or even impossible to theoretically study the full collision process starting from the interaction region to the detector. Different types of projectiles and collisional processes can be used for removing one or more electrons of a molecular system and leading to its dissociation. The most important ones are: low energy ions by charge exchange from the target to the projectile [1,2], photons with photoionization [3], or electrons with electron-impact ionization of the target [4,5]. Several theory versus experiment comparisons have been successfully carried out in the past but, as far as we know, nothing exists in the case of electrons. Nowadays, modeling from first principles of the fragmentation dynamics induced by light projectiles impacting on molecular species constitutes a real theoretical challenge. Indeed, in principle one has to simulate on equal footing the electron collision dynamics and the atomic dynamics and this over a long time, typically of the order of few microseconds that corresponds to the time-of-flight used in the experiment. At present, this complete description is not available. However, due to the strong separation of time scales between the electronic and nuclear motion, the dissociative ionization of a molecule by electron impact may be considered as resulting from two independent and successive processes. The fast collision process leads to the creation of

a vacancy in the molecular ion, putting the molecule in a doubly charged state. This specie subsequently undergoes a fragmentation reaction on a longer time scale. In this work we assume that the Franck-Condon principle is valid for electron impacts, whatever the incoming energy. Both the collisional process (ionization dynamics) and the dissociation dynamics are modeled thanks to the use of *ab initio* quantum mechanical methods using no adjustable parameters. The interest for this issue goes far beyond the case of molecular species. Indeed, the present theoretical methodology may be employed for studying larger systems such as biomolecules [6] or atomic clusters [7].

In the present paper electron-impact dissociative ionization of the HDO^+ molecular ion is investigated, both experimentally and theoretically. Absolute inclusive partial cross sections are measured in a crossed beam setup for the production of the OD^+, OH^+, and O^+ fragments. Partial dissociative ionization cross sections are deduced. The isotopic ratio OD^+/OH^+ is obtained from the experiment and calculated using the above-mentioned theoretical picture and taking into account the internal energy of the molecule before the collision.

II. EXPERIMENT

In the animated crossed electron-ion beams method [8], which applied for this experiment [4], the HDO^+ molecular ion beam of well-defined energy (3–4 keV) interacts at right angles with the electron beam of tunable energy (from a few electron volts up to 2.5 keV). The ion beam is produced in an ECR ion source filled with a mixture of H_2O, HDO, and D_2O vapors. Product ions are separated from the primary ion beam by using a double focusing 90° magnetic analyzer. Product ions are further deflected by a 90° electrostatic spherical deflector and directed onto a channeltron detector [4]. In this method the electron beam is swept across the ion beam in a linear motion at a constant velocity u so that the measured cross section σ_m is related to the total number of events K produced during one complete electron beam movement by

$$\sigma_m = \frac{uK}{I_e I_i \gamma} \frac{v_e v_i q_i e^2}{\sqrt{v_e^2 + v_i^2}}, \tag{1}$$

where γ is the detector efficiency, I_e and I_i, e and $q_i e$, and v_e and v_i are the electron and ion beam current intensities, and the charges and velocities of electrons and ions, respectively. Assuming $m_i \gg m_e$, the interaction energy E (eV) is given by

$$E = V_e + \frac{m_e}{m_i}(q_i V_i - V_e), \tag{2}$$

where V_e and V_i and m_e and m_i are the acceleration voltages and masses of electrons and target ions, respectively. Electron-impact cross section measurements are performed for dissociation of HDO^+ to form the OD^+, OH^+, O^+, and D^+ species. Due to kinetic energy release (KER) affecting the dissociation fragments, velocity distributions exceed the magnetic analyzer acceptance. To put cross sections on an absolute scale, the cross section is first measured as a function of the analyzer magnetic field. Next, the velocity distribution is computed from this apparent cross and the absolute cross section is obtained by integrating the distribution over the whole velocity range [5].

The electron energy is corrected for contact potentials by measuring accurately the appearance potential of a well-known physical process (single ionization of an atomic species) by comparing this result to the ionization threshold of reference. The collision energy is estimated with an accuracy of ±0.5 eV and the total uncertainty affecting absolute cross sections is calculated to be ±10% around the maximum. Possible fragments resulting from dissociative ionization of the HDO^+ target are OH^+/D^+, OD^+/H^+, O^+/HD^+, and $O/H^+/D^+$. In case of subsequent dissociation of the molecular fragments, one neutral atom is ejected, forming the triplets $O^+/D^+/H$, $O^+/H^+/D$, and $O/D^+/H^+$. We measured the absolute partial inclusive cross sections of OH^+, OD^+, and O^+, the H^+, D^+, and neutral O channel being not considered. Around the maximum we obtained $\sigma_{OD^+} = (7.9 \pm 0.3) \times 10^{-17}$ cm^2 and $\sigma_{OH^+} = (2.5 \pm 0.1) \times 10^{-17}$ cm^2 for the production of OD^+ and of OH^+, respectively. In the present experiment the detected fragment ions may result from dissociative excitation or ionization and a specific procedure is developed to separate these contributions [4]. Finally, absolute dissociative ionization cross sections are calculated to be $\sigma_{OD^+} = (5.68 \pm 0.3) \times 10^{-17}$ cm^2 and $\sigma_{OH^+} = (2.02 \pm 0.1) \times 10^{-17}$ cm^2 for the production of OD^+ and of OH^+, respectively (see Fig. 1 upper panel). The partial cross sections underline an important isotopic effect favoring the OD^+ channel over the OH^+ channel. The isotopic ratio, defined as the ratio of σ_{OD^+} to σ_{OH^+}, is observed to be almost constant in the 30–2500 eV energy range, about (3.1 ± 0.2) on average (see Fig. 2). According to the above-mentioned classical dynamics, the light particle

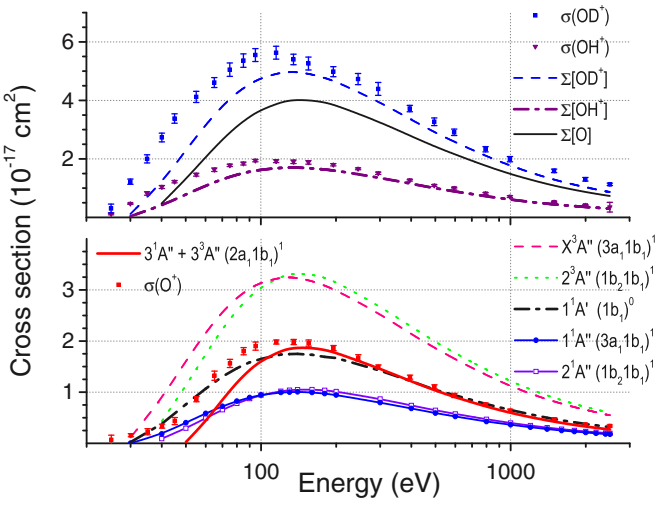

FIG. 1. (Color online) Upper panel: Squares and triangles with error bars: Experimental electron-impact dissociative ionization cross sections for the production of OD^+ and OH^+. Dashed and dashed-dot lines are their theoretical equivalents at $T = 2000$ K, with $\Sigma[\alpha]$ being defined in Eq. (4). Solid line: Theoretical cross section for the production of O. Lower panel: Computed ionization cross sections of vertical transitions from the ground state $\tilde{X}\,^2B_1$ of HDO^+ to the first seven states of HDO^{2+} (an electron is removed from one of the four highest molecular orbitals, as indicated in the inset). Solid squares with error bars: Experimental cross section for the production of O^+. Solid line: Theoretical cross section corresponding to the creation of a vacancy in the $2a_1$ orbital.

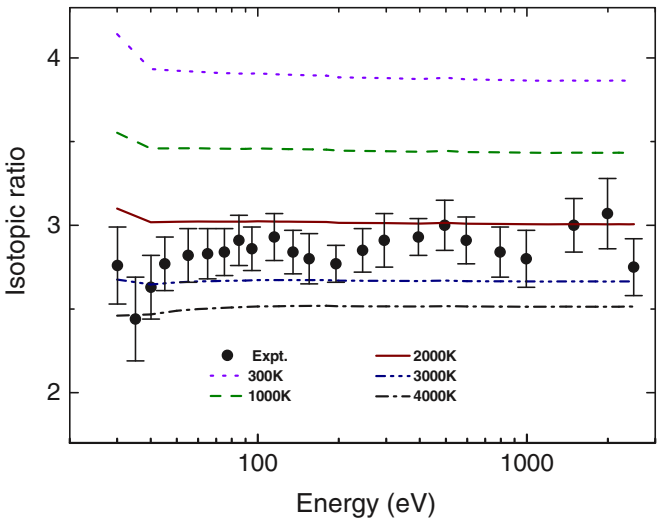

FIG. 2. (Color online) Electron-impact dissociative ionization of HDO^+: Isotopic ratio $\sigma_{OD^+}/\sigma_{OH^+}$ (full dots with error bars) versus the electron-impact energy. The other curves correspond to the theoretical predictions $\rho(E,T)$ for several vibrational temperatures.

ejection should prevail with respect to the heavy one. The present result supports this argument, as the lightest particle H^+ is associated with OD^+ formation while D^+ is associated with OH^+ production, a result which is qualitatively and quantitatively very similar to the one observed for D_2H^+ [5].

III. ELECTRON-IMPACT IONIZATION CROSS SECTIONS

The presence of two free electrons in the final state complicates the boundary conditions and makes a first-principles computational treatment of the electron-impact ionization process extremely difficult. Although some excellent work has been performed on simple atoms, computational treatments of electron-impact ionization of molecules have mostly been restricted to elementary models [9] based on the binary encounter and Born-Bethe approximations. In recent years we developed a theoretical modeling based on *ab initio* methods that allows us to compute electron-impact ionization cross sections [10]. The associated calculations are generally very demanding in computer time but do not rely on any fitting parameters. More importantly, this kind of model allows us, from the knowledge of the cationic molecular orbitals, to evaluate the ionization probabilities of the different states of the molecular dication which participate in the fragmentation dynamics.

The collision process is treated within the framework of the nonrelativistic first Born approximation (FBA). Quantum chemical computations of the molecular wave function were conducted using a similar approach than in our previous work for water [11], where we discussed the quality of the methods. The geometry of the HDO^+ ion was optimized at the unrestricted open-shell (doublet) Hartree-Fock level with a second-order corrections (MP2) method [12] for the electronic correlation energy. In the calculations the wave function was computed using the augmented, correlation-consistent, polarized-valence quadruple-zeta basis set (aug-cc-pvQZ) of Dunning and co-workers [13]. This basis set consists of Gaussian-type orbitals with contraction $(13s\,7p\,4d\,3f\,2g)/[6s\,5p\,4d\,3f\,2g]$. For convenience we use Cartesian d, f, and g functions. The total number of atomic orbitals for water is 215 with 241 primitive Gaussians. Minimum energy was obtained for a geometry having OH distances of $1.884a_0$ and $\widehat{HOD}$ angle of 109.57°. Afterwards, the wave function of the system was recomputed using a restricted open-shell Hartree-Fock method and the same basis set. All the computations have been carried out using the GAUSSIAN03 program [14]. The molecular wave function is subsequently converted to a single-center expansion by using partial-wave expansion techniques [15] and cross sections are computed using a method developed for calculating multiply differential and total cross sections for electron-impact ionization of molecules [10]. In addition, we followed the efficient procedure developed by Bartlett and Stelbovics [16] for the calculation of the electron-impact total ionization cross sections of neutral atoms, which consists of orthogonalizing the continuum Coulomb wave describing the ejected electron to the orbital of the molecule that is considered. Let us stress that this orthogonalization significantly improves the agreement with experimental data for the noble-gas series compared to previous Born models. Particle exchange is treated using the so-called Born(b) approximation described in [17]. Finally, we have neglected effects coming from molecular vibrations since this approximation is a common one in gas-phase studies [18].

The coupling of spins of the incident electron and the H_2O^+ target in the $\tilde{X}\,^2B_1$ ground state, which the electronic configuration $(1a_1)^2(2a_1)^2(1b_2)^2(3a_1)^2(1b_1)^1$, having thus a hole in the $1b_1$ molecular orbital, will result into four states characterized by the total spin $(S=0, M_s=0)$ and $(S=1, M_s=0,\pm1)$. Their associated wave functions are expressed in a combination of Slater determinants constructed with the appropriate spin orbitals [19]. We consider only states where an electron has been removed from one of the four highest molecular orbitals, as the lowest orbital $(1a_1)$ leads essentially to an Auger decay [20]. Starting from the highest orbital we have the singlet $1\,^1A'\,(1b_1)^0$, the triplet $X\,^3A''$, and singlet $1\,^1A''\,(3a_1)^1(1b_1)^1$, the triplet $2\,^3A''$ and singlet $2\,^1A''\,(1b_2)^1(1b_1)^1$, and the triplet $3^3A''$ and singlet $3^1A''\,(2a_1)^1(1b_1)^1$. Together with the scattered and ejected electron, we construct the final states with total spin $S=0,1$ for each dicationic state. The spin multiplicity of each state is thus implicitly taken into account. The ionization potentials of the dicationic PES are taken from [21] and therein references (see also Table I).

IV. INTERNAL STATES OF HDO^+ BEFORE ELECTRON-IMPACT IONIZATION

The fragmentation process of a HDO^{2+} dication can be efficiently simulated by means of a three-body classical dynamics on fitted potential energy surfaces (PESs) of the dication and allows us to compute, for those PESs, the proportion of dissociation channels into two (H^+/OD^+ and D^+/OH^+) or three fragments [21]. The outcome of the dissociation dynamics on a given dicationic PES strongly depends on the initial conditions (positions and momenta of the three atoms) and thus on the electronic and vibrational state of the HDO^+ cation before the electron impact. Since the latter

TABLE I. Dissociation probabilities (in percent) of each channel α and for each PES j of the dication that is accessible from the cationic ground state $\tilde{X}\,^2B_1$ (left, $P_j[\alpha]$) and the first excited state $\tilde{A}\,^2A_1$ (right, $P_j^*[\alpha]$) of HDO^+ at $T = 2000$ K. $V_{\rm ion}$ stands for the vertical transition energies from the cationic states at their equilibrium geometry taken from [21].

$\tilde{X}\,^2B_1$ ($T = 2000$ K)		$V_{\rm ion}$ (eV)	OD^+	OH^+	O^+	O	$\tilde{A}\,^2A_1$ ($T = 2000$ K)		$V_{\rm ion}$ (eV)	OD^+	OH^+	O^+	O
$1\,^1A'$	$(1b_1)^0$	28.27	68	31	–	1	$2\,^1A'$	$(3a_1)^0$	28.99	67	32	–	1
$X\,^3A''$	$(3a_1)^1(1b_1)^1$	27.02	78	20	–	2	$X\,^3A''$	$(3a_1)^1(1b_1)^1$	24.87	65	35	–	–
$1\,^1A''$		29.48	80	18	–	2	$1\,^1A''$		27.18	68	31	–	1
$2\,^3A''$	$(1b_2)^1(1b_1)^1$	31.21	3	<1	–	97	$1\,^3A'$	$(1b_2)^1(3a_1)^1$	32.76	6	1	–	93
$2\,^1A''$		32.97	5	<1	–	95	$3\,^1A'$		34.43	9	1	–	90
$3\,^3A''$	$(2a_1)^1(1b_1)^1$	48	–	–	100	–	$4\,^3A'$	$(2a_1)^1(3a_1)^1$	48	–	–	100	–
$3\,^1A''$		48	–	–	100	–	$4\,^1A'$		48	–	–	100	–

are not measured in the experiment, we assume the following estimates:

(i) We suppose that the ionization process in the ECR source is dominated by a vertical transition from the neutral HDO to cationic states. Determining the rotational and vibrational temperatures of the molecular ions in the collision region is not a trivial task. Indeed, it strongly depends on the formation mechanism of the molecular ions and their cooling between the time of production in the source and the time of interaction with the electron beam. Concerning this issue, for molecular ions other than hydrogen, we can certainly make reference to the experimental work of [22]. According to these authors, the HeH^+ rotational temperature ranges from 2400 K to 3200 K and 2800 K for the vibrational temperature.

(ii) Analyzing the PESs of the first ten electronic states of HDO^+, one notices that only the first three lowest states, $\tilde{X}\,^2B_1$, $\tilde{A}\,^2A_1$, and $\tilde{B}\,^2B_2$, are mainly nondissociative in the Franck-Condon area of the equilibrium geometry of neutral HDO [23]. The second excited electronic state $\tilde{B}\,^2B_2$, which is connected to the first excited state $\tilde{A}\,^2A_1$ through a conical intersection, has a short lifetime of about 10 ps [24], much shorter than the extraction time of the ECR source, which is estimated to be about 6 μs. In addition, a vertical transition to the second excited state $\tilde{B}\,^2B_2$ state places the ion in a state which lies above the dissociation limit of H^+/OH and H/OH^+ of the $\tilde{A}\,^2A_1$ state [25]. For the other seven states, this Franck-Condon area is rather steep and leads to dissociation of the molecule. These states have a smaller cross section than the three lower lying states as they are obtained by an ionization plus an excitation of a second valence electron. We thus propose in the following to focus only on the first two cationic states.

(iii) The relative population of the two cationic species ($g \equiv \tilde{X}\,^2B_1$) and ($e \equiv \tilde{A}\,^2A_1$) created in the ECR source by electron-impact ionization of HDO can be estimated by using the well known approximate Thomson's scaling law $V_{\rm ion}^{-2}$ for ionization cross section [26], where $V_{\rm ion}$ is the ionization potential of the molecule. Since $(V_{\rm ion})_e = 14.6$ eV and $(V_{\rm ion})_g = 12.3$ eV [23], $\sigma_g/\sigma_e = [(V_{\rm ion})_e/(V_{\rm ion})_g]^2 \simeq 1.4$ and $\alpha_e(0) = 0.7\alpha_g(0)$, where $\alpha_i(t = 0)$ means the population of specie i at the instant of ionization in the ECR source. The first cationic excited state (e) decays to the ground state (g) with a lifetime of $\tau_r = 10.5$ μs [27]. According to the experimental setup, the time-of-flight between the ECR source and the collision chamber can be estimated to be $\tau_{\rm tof} = 13$ μs leading to the ratio $\alpha_e(\tau_{\rm tof})/\alpha_g(\tau_{\rm tof}) = 0.135$ at the collision point. This implies that about 12% of the ions in the collision chamber are in the $\tilde{A}\,^2A_1$ excited state and 88% are in their ground state. The large difference between the equilibrium geometry of these two states suggests significant vibrational excitation for the cationic ground state formed by decay.

V. DISSOCIATION DYNAMICS AND ISOTOPIC RATIO

As the first two states of HDO^+ have different electronic configurations, they lead to different accessible dicationic states when removing one electron from one of the four highest molecular orbitals. In the following we focus on the cationic ground state, but the discussion also holds for the cationic excited state. Removing one electron from one of the three valence orbitals $1b_2$,$3a_1$,$1b_1$, leads to dicationic states that dissociate into OH^+/D^+, OD^+/H^+, or $O/H^+/D^+$. The probability $P_j[\alpha](T)$ of each channels α is calculated by performing 10^5 classical molecular dynamic on each fitted PES j and by recording the number of times the molecule ends up in one of the three dissociation channels $\alpha = \{OD^+, OH^+, O\}$. Initial positions and velocities of the three atoms are sampled according to the temperature (T) dependent phase-space distribution function $f(T)$ of each vibrational mode.

The three eigenmodes Q_i and eigenfrequencies ω_i of HDO^+ are calculated by diagonalizing the Hessian matrix, which is computed using the PES of [28] for the cationic ground state and its excited state. Moreover, we have assumed that for a temperature up to 1/3 eV (≈4000 K) the potential well of a vibrational mode is harmonic. From the model of a quantum harmonic oscillator at thermal equilibrium, we obtain the density matrix and energy $\frac{1}{2}\hbar\omega_i(T) = \frac{1}{2}\hbar\omega_i \coth(\frac{\hbar\omega_i}{2k_BT})$ of each mode i. The classical distribution of the phase-space coordinates $(x,\dot{x})$ for the ith eigenmode is then obtained by the Wigner transform of the density matrix [29], yielding

$$f_i(T;x,\dot{x}) = N \exp\left(-\frac{x^2\mu_i\omega_i^2}{\hbar\omega_i(T)}\right)\exp\left(-\frac{\dot{x}^2\mu_i}{\hbar\omega_i(T)}\right), \quad (3)$$

where N is the normalization constant and μ_i is the reduced mass of the ith eigenmode. The effect of the temperature is to broaden the distribution for both coordinates, resulting in larger vibrational amplitudes and velocities. Details about the

initial conditions, dissociation dynamics, and the eight fitted dicationic PESs are given in [21,30].

The probabilities have been calculated for several vibrational temperatures ranging from $T = 300$ K to $T = 4000$ K. The case $T = 2000$ K is reported in Table I, left for the cationic ground state and right for its excited state. Removing one electron from the $(2a_1)$ molecular orbital puts the ion onto the triplet $3\,^3A''$ or singlet $3\,^1A''$ state, which are expected to feed exclusively the O^+ channel. Therefore, we assign $P[O^+] = 1$ to this state independently from temperature. This is corroborated by the excellent agreement between the experimental O^+ cross section and the cumulated cross section of those states (see lower panel of Fig. 1).

One can now calculate the total electron-impact cross section $\Sigma[\alpha]$ of a channel $\alpha = \{OD^+, OH^+, O^+, O\}$ as functions of the electron-impact energy E and the vibrational temperature T of HDO^+,

$$\Sigma[\alpha] = \sum_j (1-\beta)\sigma_j(E)P_j[\alpha](T) + \beta\sigma_j^*(E)P_j^*[\alpha](T), \quad (4)$$

where j runs over all accessible dicationic states. The value $\beta \sim 0.12$, as discussed previously, corresponds to the proportion of excited HDO^+ ions in the collision chamber. σ_j is the ionization cross section of a transition to the dicationic state j (shown in Fig. 1). The asterisk indicates the contributions from the excited cationic state. The equilibrium geometry of the $\tilde{A}\,^2A_1$ being of $D_{\infty,h}$ symmetry, the orbitals $1b_1$ and $3a_1$ play the same role and we consider $\sigma_j^* = \sigma_j[(V_{\rm ion})_j/(V_{\rm ion})_j^*]^2$. In Fig. 1, $\Sigma[OD^+]$ and $\Sigma[OH^+]$ cross sections are compared to the experimental data. As for the O^+ channel, we find an excellent agreement in the higher energy range. However, the theoretical values underestimate the experimental cross sections in the lower energy range. This discrepancy appearing at low impact energy is not surprising. Indeed, we are using a collisional model based on the first Born approximation. The latter is supposed to be valid only at relatively high impact energy. This model may be improved by describing the incoming and ejected electrons by distorted waves. These possible modifications constitute a real theoretical challenge in the field of molecular collisions. The full black curve represents the cross section for the production of neutral O. This channel is mainly fed by the dicationic states obtained by removing an electron from the binding $1b_2$ molecular orbital. From Eq. (4) we deduce the isotopic ratio ρ as functions of the electron-impact energy E and vibrational temperatures T as $\rho(E,T) = \Sigma[OD^+](E,T)/\Sigma[OH^+](E,T)$. The isotopic ratio is an observable that is extremely sensitive to the vibrational energy of the HDO^+ ion as it zooms on the Frank-Condon area of the dicationic PESs. The experimental and theoretical isotopic ratios are shown in Fig. 2. This comparison indicates that the ECR ion source produces an ion beam with a temperature between 2000 and 3000 K which is compatible with typical characteristics of ECR ion sources. Regarding the vibrational energy of the $\tilde{X}\,^2B_1$ cationic state (bending 1200 cm^{-1}, symmetric stretching 2000 cm^{-1}, and asymmetric stretching 3200 cm^{-1}), it means that a few vibrational modes are actually populated at about 2500 K.

VI. CONCLUSIONS

We have presented a complete theoretical and experimental study of the dissociative ionization of HDO^+ by electron impact. Experimental absolute partial inclusive cross sections for the production of OD^+, OH^+, and O^+ are reported and compared successfully to theoretical predictions. The latter have been obtained using *ab initio* methods employing no adjustable parameters. We compute electron-impact ionization cross section of the cationic states which are present in the collision chamber leading to the seven lowest dicationc states. Classical molecular dynamics simulation was then performed on the different dicationic PESs in order to obtain the probability of each dissociation channel as a function of the vibrational temperature. The three measured channels were directly compared to theoretical predictions, highlighting an overall good agreement. The neutral oxygen channel which is not measured in the experiment is predicted to contribute at the level of 30% of the total ionization cross section. From the OH^+ and OD^+ channels we computed the isotopic ratio for several temperatures. The comparison with the experiment data shows that a good agreement is only possible when the ECR source temperature is taken into account in the theoretical modeling. The predicted vibrational temperature of the ion beam is found to be about 2500 K which is fully compatible with characteristic values of ECR ion sources. These agreements support the main physical assumption of our model namely: the temporal separation between the electron-impact ionization (fast process) and the dissociation (slow process) which is justified by the very different time scales associated with these two processes. What is remarkable is that this latter hypothesis allows us to produce quantitative results through the use of Eq. (4). This study shows a nice example where both the experiment and the theory are hindered by incomplete knowledge, but where a combined analysis allows us to reconstruct the missing information. Finally, the proposed theoretical methodology may be beneficially employed for studying fragmentation induced by electron impact of larger molecular systems such as biomolecules or atomic clusters.

[1] A. Rentenier *et al.*, Phys. Rev. Lett. **100**, 183401 (2008).

[2] A. Lawicki *et al.*, Phys. Rev. A **83**, 022704 (2011).

[3] M. Murakami *et al.*, Chem. Phys. Lett. **403**, 238 (2005).

[4] J. Lecointre *et al.*, J. Phys. B **39**, 3275 (2006).

[5] P. Defrance *et al.*, J. Phys. B **44**, 075202 (2011).

[6] I. I. Shafranyosh, M. I. Sukhoviya, and M. I. Shafranyosh, J. Phys. B **39**, 4155 (2006).

[7] D. Hathiramani, K. Aichele, W. Arnold, K. Huber, E. Salzborn, and P. Scheier, Phys. Rev. Lett. **85**, 3604 (2000).

[8] The term "animated beams" appeared for the first time in the title of the article: F. Brouillard and P. Defrance, Phys. Scr. **T3**, 68 (1983).

[9] Y.-K. Kim and M. E. Rudd, Phys. Rev. A **50**, 3954 (1994).
[10] C. Dal Cappello, P. A. Hervieux, I. Charpentier, and F. Ruiz-Lopez, Phys. Rev. A **78**, 042702 (2008).
[11] H. Hafied, P. A. Hervieux, I. Charpentier, and F. Ruiz-Lopez, Chem. Phys. Lett. **439**, 55 (2007).
[12] C. Moller and M. S. Plesset, Phys. Rev. **46**, 618 (1934).
[13] R. A. Kendall *et al.*, J. Chem. Phys. **96**, 6796 (1992).
[14] M. J. Frisch *et al.*, GAUSSIAN03, Revision C.02, Gaussian, Inc., Wallingford, CT, 2004.
[15] K. Kaufmann and W. Baumeister, J. Phys. B **22**, 1 (1989).
[16] P. L. Bartlett and A. T. Stelbovics, Phys. Rev. A **66**, 012707 (2002).
[17] M. R. H. Rudge, Rev. Mod. Phys. **40**, 564 (1968).
[18] P. Weck, B. Joulakian, J. Hanssen, O. A. Fojón, and R. D. Rivarola, Phys. Rev. A **62**, 014701 (2000).
[19] F. Boudali, B. Najjari, and B. Joulakian, J. Phys. B **33**, 2383 (2000).
[20] M. O. Krause, Phys. Chem. Ref. Data **8**, 307 (1979).
[21] B. Gervais *et al.*, J. Chem. Phys. **131**, 024302 (2009).
[22] W. Ketterle, A. Dodhy, and H. Walther, J. Chem. Phys. **89**, 3442 (1988).
[23] F. Schneider *et al.*, J. Chem. Phys. **105**, 7560 (1996).
[24] D. Dehareng *et al.*, J. Chem. Phys. **78**, 1246 (1983).
[25] K. H. Tan *et al.*, Chem. Phys. **29**, 299 (1978).
[26] J. J. Thomson, Philos. Mag. **23**, 449 (1912).
[27] G. R. Möhlmann *et al.*, Chem. Phys. **31**, 273 (1978).
[28] T. R. Huet *et al.*, J. Chem. Phys. **97**, 5977 (1992).
[29] M. Hillery, R. F. O'Connell, M. O. Scully, and E. P. Wigner, Phys. Rep. **106**, 121 (1984).
[30] S. Legendre *et al.*, J. Phys. B **38**, L233 (2005).